Visual Inspection Of Machined Parts *

Bharath R. Modayur †, Linda G. Shapiro ‡and Robert M. Haralick †

†Department of Electrical Engineering, FT-10
‡Department of Computer Science & Engineering, FR-35
University of Washington
Seattle WA 98195
U.S.A.

Abstract

Although many special purpose inspection systems have been developed, general purpose systems utilizing CAD models of the parts are still in the research stage. While it is easy to define ad hoc algorithms for inspection, it is much more difficult to justify the algorithms with solid theory. In this paper we describe a CAD-model-based machine vision system for dimensional inspection of machined parts, with emphasis on the theory behind the system. The original contributions of our work are: 1) the use of precise definitions of geometric tolerances suitable for use in image processing, 2) the development of measurement algorithms corresponding directly to these definitions, 3) the derivation of the uncertainties in the measurement tasks, and 4) the use of this uncertainty information in the decision-making process. Our initial experimental results have verified the uncertainty derivations statistically and proved that the error probabilities obtained by propagating uncertainties are lower than those obtainable without uncertainty propagation.

1 Introduction

The problem of automating industrial inspection tasks is an interesting and challenging one. Modern design techniques are performed via computer and produce a geometric model of the part being designed. Three-dimensional graphics techniques can be applied to this model to generate various views of the object for the designer to look at. It is clearly desirable to develop machine vision techniques to inspect the finished (or partially finished) part.

Many special purpose inspection systems have been developed; some are even in use on the factory floor. General purpose systems are still in the research stage. While it is easy to define *ad hoc* algorithms for inspection, it is much more difficult to justify the algorithms with solid theory. This section motivates our approach to the problem and discusses related work. Section 2 starts with a discussion on conventional and geometric tolerancing schemes, defines the simulated datum features used in this work, and explains the construction of these datum features. Section 2 also defines the different tolerance types and describes the algorithms that carry out the inspection tasks. Section 3 explains the need to propagate uncertainty information in measurement tasks and carries the reader through one task, namely measurement of straightness of edges. Section 4 explains the relevant image processing operators and sequences used in extracting the required features from an image. Section 5 discusses the experiments and results, and we conclude with section 6.

1.1 Statement of the Problem

The purpose of tolerance specifications is to enable us to decide whether a manufactured part is acceptable. This will be the case if all its features (edges and vertices in our work) are within the corresponding tolerance zones, the size, shape and orientation of which are dictated by the tolerance assertions. In our present work, we consider only edge and vertex features. Assume there is 1) a solid model M with vertex set V^M and edge set E^M and 2) a part P to be inspected with vertex set V^P and edge set E^P. This part P has a one-to-one feature correspondence with the model M. It will pass the inspection test if all its features in sets V^P and E^P satisfy the tolerance specification(s) imposed on the corresponding features of the ideal model M. The pose and orientation of the part P is known with some uncertainty. We have one or more images

*This research was supported by the National Science Foundation under grants DMC-8714809 and IRI-9023977 and by the Washington Technology Center.

0-8186-2855-3/92 $3.00 ©1992 IEEE

of the part. The problem is to determine whether the part P passes the inspection test.

1.2 Motivation for our Work

An inspection task can be broken down into three stages: the object recognition/pose determination stage, the inspection stage, and the decision-making stage. The output of the recognition stage is the identity of the object being inspected and a transformation matrix. In the inspection stage, image processing, feature extraction, and measurement routines are employed to access and test those features required by the inspection task. The decision-making stage determines whether the manufactured part being inspected is satisfactory ("in spec") or not ("out of spec"). Since a real part is never perfect and a real image is never noise free, the position and orientation obtained from the recognition stage have uncertainty associated with them. Noise in the image creates uncertainty in the estimated attributes of the entities obtained as a result of image processing.

Our beliefs about the need for propagation of uncertainty are an important factor in this work. A second key factor that has motivated the work is the need to have precise definitions for the various types of tolerances and the need to have measurement algorithms that perform a measurement task *exactly* the way it is laid out in the tolerance definitions. The one common inadequacy of a number of related works has been the fact that the measurement algorithms do not follow the guidelines set up in the formal definition of tolerances. In this work, we try to bridge the gap and make the measurements correspond exactly to the definition of tolerances.

1.3 Related Literature

Though there is an abundance of literature in the area of automatic visual inspection for specific domains (e.g: solder joints, printed circuit boards, light bulb filaments, etc.), literature on inspection systems (specifically CAD-based) for general machine parts is hard to come by.

Requicha [7] was the first to lay down a formal theory of tolerancing. We draw on the ideas in this seminal work and the guidelines prescribed in the ANSI standards [1] to set up formal definitions of the various tolerances. Park *et al* [5] discussed issues in developing an automated inspection system with emphasis on achieving an integrated CAD-Vision model, not on the tolerance theory or the measurement tasks. Other inspection systems have been described by [8] and [2]. Although a number of coordinate measurement machine (CMM) vendors claim to have solved the inspection problem, they work by fitting surfaces and curves to image data and inspecting the parameters of the fit. This, however, is not what the industrial standards prescribe.

2 Tolerancing Schemes

Conventional tolerancing schemes resort to excessive use of implicit datums, leaving the designer to resolve inherent ambiguities. Lack of explicit datums leads to varying interpretations of what the designer really intended. Geometric tolerancing, which is widely used in industry, is well-defined in the ANSI standards. In this scheme, use is made of explicit datum features. We make a simple extension to the guidelines laid out in the ANSI standards and the formal theory proposed by Requicha [7] to enable the imposition of tolerances on two-dimensional object features that are observable in an image. We decide if an object feature is acceptable or not depending on whether the feature lies within zones created by offsetting the feature's ideal shape.

It is not always possible to define dimensions exactly on an imperfect object feature. Geometric tolerancing employs "simulated datum features" to overcome this problem. A *simulated datum feature* is a perfectly formed geometric entity that is associated with an imperfectly shaped, manufactured object feature. Measurements made using imperfect object features are not well-defined/meaningful. The standards suggest the use of simulated datum features (henceforth referred to as just datum features) in order to make the measurements well-defined. Thus, our inspection system must associate with imperfect, real features, corresponding perfectly-formed features so that measurements can be made.

We consider five geometric features in our inspection tasks. They are: straight lines, circles with the material side external to the circle, circles with the material side internal to the circle, rectangles with the material side external to the rectangle, and rectangles with the material side internal to the rectangle. These correspond to the two-dimensional counterparts of a planar feature, a cylindrical slot, a cylindrical part, a rectangular slot, and a rectangular part, respectively. In order to implement our measurement tasks, datum features have to be associated with these five geometric features.

2.1 Datum Features - Definitions

Planar Object Features: Planar object features in 3D are just planar surfaces of the part. A popular industrial practice used to associate a planar datum to an irregular surface is to let a known planar object rest on the irregular surface. We are going to inspect edges which are 2D projections of planar surfaces. The simulated datum feature for an edge is a straight line positioned so as to minimize the integral sum of distances between points on the edge to the straight line.

Cylindrical Parts and Slots: The 2D profile of a cylindrical part is a circle with the material side internal to the circle. The associated simulated datum is the smallest circumscribing circle. The 2D counterpart of a cylindrical slot is a circle with the material side external to the circle. In ANSI terminology, a cylindrical slot is an internal feature. The associated simulated datum is the largest inscribing circle.

2.2 Datum Features - Construction

It is not enough to merely define datum features. In addition, we must specify how these features are to be constructed, and their constructions must be suitable for implementation in the digital image domain. This section deals with the actual construction of the different datum features we discussed before.

Straight Line Datum: According to ANSI standard Y14.5M, where a nominally flat surface (in two dimensions, a straight line) is specified as a datum feature, the corresponding datum is simulated by a plane (a straight line in 2D) contacting the high points of the surface. This gives us a simulated datum that is physically and geometrically meaningful and the datum is "close" to the irregular surface in some sense. Refining this idea further, we can require that the integral sum of distances from the simulated plane to the irregular surface be a minimum. This makes the datum plane "the closest" to the actual manufactured surface. Thus, in two-dimensions, we have the following problem.

Given N points in 2 space, construct a supporting line L[1] to these N points such that the sum of perpendicular distances from the N points to this line L is a minimum. The following theorem gives the solution to this problem.

Theorem:
Given N points in 2 space, the supporting line that minimizes the sum of perpendicular distances to these N points passes through an edge of the convex hull of the N points.

Thus, given N points in 2 space belonging to an edge, the simulated datum straight line is constructed in the following way. Construct the convex hull CH_N. The supporting line that minimizes the sum of perpendicular distances is an edge E_i of the hull. So, we can compute the sum of perpendicular distances for all the edges of CH_N. Choose the edge yielding the lowest sum of distances. This is the required straight line datum.

Circular Parts and Slots: The required simulated datum is the smallest circumscribing circle to the set of edge points constituting the circle. The simulated datum is the largest inscribing circle for the set of edge points constituting the slot outline.
Constructing the smallest circumscribing circle and the largest inscribing circle for a set of 2D data points is a well-defined computational geometry problem [6].

2.3 Tolerance Definitions and Measurements

In this section, we will define a few of the tolerance types and give a brief account of the algorithms to make those tolerance measurements on an object feature.

Straightness of an Edge

Definition: An edge with a straightness tolerance T_s conforms to the specification if it can be enclosed completely by two parallel lines at a separation less than T_s.
Measurement: We check for the straightness in the following way. The required simulated datum feature (in this case, a straight line) is first constructed. This datum line is then translated until all the edge points are on or between the simulated datum and this translated version. If the distance between these two parallel lines is less than T_s, the edge conforms to the straightness specification.

Angularity of Edges

Definition: Let the ideal angle between two edges be θ_{id} and let the angular tolerance be specified by T_a. The two edges satisfy the angular tolerance, if the angle between the two associated simulated datum features is θ_{obs}, satisfying $\theta_{id} - T_a/2 \leq \theta_{obs} \leq \theta_{id} + T_a/2$.
Measurement: We construct the simulated datum

[1] We require L to be a supporting line because we want the datum to completely enclose the irregular edge.

features associated with the two edges as outlined before. Then we measure the angle between the two resultant straight lines. The measured angle must to lie within the interval $[\theta_{id} - T_a/2, \theta_{id} + T_a/2]$ for the edges to conform to the angularity tolerance.

3 Uncertainty Propagation in Measurements

A real image is seldom absolutely noise free. Noise in the image leads to uncertainties in the attributes of the entities output by image processing algorithms. Uncertainty in the lower-level image entities leads to uncertainty in the tolerance measurement tasks. To illustrate this, we will take the reader through one task, namely measurement of straightness of an edge. The derivations for variances of other measurements are similar in principle.

3.1 Noise Model

Let the true edge pixel position be denoted by (x_i, y_i). Let the observed edge pixel position be denoted by $(\hat{x_i}, \hat{y_i})$. Our model for the noisy, observed edge pixel is, $\hat{x_i} = x_i + \epsilon_i$, $\hat{y_i} = y_i + \xi_i$. where, ϵ_i and ξ_i are samples from independent distributions that are even functions [9], with mean zero and variances σ_{ϵ_i} and σ_{ξ_i}, respectively.

3.2 Datum Line Uncertainty

The simulated datum line for straight edges is the nearest-supporting line that passes through an edge L_1 of the convex hull of the edge pixels. Let us denote the end points of this hull edge by (x_1, y_1) and (x_2, y_2). We can write the line equation as $L_1 : \alpha x + \beta y + \gamma = 0$. Since, we only have noisy observations $(\hat{x_1}, \hat{y_1})$ and $(\hat{x_2}, \hat{y_2})$, the observed line parameters would be expressed as functions of $(\hat{x_2}, \hat{y_2})$.

Let us estimate the behavior of one of the line parameters α as a result of noise on the edge pixels. We will represent α by a Taylor series expansion around the true edge points (x_1, y_1) and (x_2, y_2). We can then truncate the Taylor series as an approximation and include only the linear terms. As a result

$$\begin{aligned}\hat{\alpha} &= \alpha + \frac{(y_2 - y_1)^2}{d^3}[(\hat{y_1} - y_1) - (\hat{y_2} - y_2)] \\ &+ \frac{(x_2 - x_1)(y_2 - y_1)}{d^3}[(\hat{x_1} - x_1) - (\hat{x_2} - x_2)] + \\ &\frac{1}{d}[(\hat{y_2} - y_2) - (\hat{y_1} - y_1)]\end{aligned}$$

Squaring the above equation and taking expectations on both sides results in

$$\begin{aligned}V[\hat{\alpha}] &= [V[\hat{y_1}] + V[\hat{y_2}]]\left(\frac{(y_2 - y_1)^4}{d^6} - \frac{(y_2 - y_1)^2}{d^4} + \frac{1}{d^2}\right) \\ &+ [V[\hat{x_1}] + V[\hat{x_2}]]\left(\frac{(x_2 - x_1)^2(y_2 - y_1)^2}{d^6}\right) \\ &+2\,[Cov[\hat{x_1}, \hat{y_1}] + Cov[\hat{x_2}, \hat{y_2}]] \\ &\left(\frac{(y_2 - y_1)^3(x_2 - x_1)}{d^6} - \frac{(x_2 - x_1)(y_2 - y_1)}{d^4}\right) \quad (1)\end{aligned}$$

In a similar way, we can estimate the variances of the parameters $\hat{\beta}$ and $\hat{\gamma}$ in terms of the coordinates (x_1, y_1) and (x_2, y_2). To measure the straightness of this edge, L_1, we have to find another line parallel to this datum line and such that all the edge pixels are on or between the two lines. Assume that this parallel line, L_2, passes through (x_3, y_3). The equation for L_2 is $L_2 : \hat{\alpha}x + \hat{\beta}y - (\hat{\alpha}x_3 + \hat{\beta}y_3) = 0$. The distance between the two parallel lines that should conform to the straightness tolerance is $\hat{d} = \hat{\alpha}x_3 + \hat{\beta}y_3 + \hat{\gamma}$. Since α and β are themselves functions of θ which is the angle that the line makes with the X-axis, we can rewrite d as a function of θ and γ. Proceeding with the truncated Taylor series expansion as before,

$$\begin{aligned}V[\hat{d}] &= V[\hat{\theta}][x_3 \cos\theta + y_3 \sin\theta]^2 + V[\hat{\gamma}] + \\ &2[x_3 \cos\theta + y_3 \sin\theta]Cov[\hat{\theta}, \hat{\gamma}] \quad (2)\end{aligned}$$

Equation 2 expresses the uncertainty of the straightness measurement, given the observed coordinates of the two edge pixels that support the datum line ($(\hat{x_1}, \hat{y_1})$ and $(\hat{x_2}, \hat{y_2})$) and the third edge pixel $(\hat{x_3}, \hat{y_3})$ that is farthest away from this datum line, and the variances of the observed edge pixel positions. Thus, the uncertainties in the edge pixel positions have been propagated all the way up to the measurement task.

4 Image Processing for Inspection Tasks

The image processing operators, instead of operating on the entire image, operate only in specific regions, called "search windows" where we expect features (such as edges) to lie. Given the uncertain transformation matrix and an estimate of the noise in the image, an accurate estimate of the size and position of these search windows can be obtained [4]. The first step in our image processing sequence is edge detection followed by a shrinking operation. The edge detector output is contaminated with stray noise specks, spurious edge pixels and small segments that

cannot be grouped with other segments on the basis of adjacency or orientation. Thus, a necessary step after edge detection is symbolic grouping, based on adjacency and orientation, of edge pixels to form a higher-level entity. The set of edge segments output by the grouping process is directly used by the measurement procedures. Corner pixels are obtained as a by-product of the grouping process described above. Points of high curvature on the arc segments are classified as corners.

5 Experiments and Results

We have run a preliminary set of experiments to validate our procedures. As a first step in our experiments, we checked for the accuracy of the variance formulas derived for the various measurement tasks. We employed a statistical testing procedure for this purpose, taking the straightness measurement as an example task.

In order to test whether $\sigma^2_{\hat{d}}$, the variance of the straightness measure $\hat{d}$ is equal to $V[\hat{d}]$, the analytic formula derived for, the null and alternate hypotheses were formulated to be

$$H_0 : \sigma^2_{\hat{d}} = V[\hat{d}]$$
$$H_a : \sigma^2_{\hat{d}} \neq V[\hat{d}],$$

and the test statistic to be

$$Test = \frac{\sigma^2_{\hat{d}} - V[\hat{d}]}{\sigma^2_{\sigma^2_{\hat{d}}}}.$$

Since the distribution of $\sigma^2_{\hat{d}}$ is not known, we approximate the mean and variance of $\sigma^2_{\hat{d}}$ by the experimental mean straightness measure variance and the mean variance of the straightness measure variance, respectively. The statistical test was carried out with the significance level α=0.05, corresponding to a value of ± 1.96 for a normalized Gaussian random variable. Thus the null hypothesis would be accepted if the test statistic were between ± 1.96.

Figure 1 shows the result of the statistical test for a line oriented at 45^0, with perpendicular distance to the farthest edge point being 35 pixels. The statistical test value fell below the significance level when the distance between the two points fell below 12. Thus, for the linearization approximations made in the variance derivations to hold, the two points that support the datum line must be separated by at least four standard deviations (of the noise).

The second stage of our experiments focused on determining the performance of the measurement algorithms with and without error propagation. We again tested the straightness measurement algorithm. Our experimental object, shown in Figure 2, was modeled using PADL-2 and machined on a CAMM-3 modeling machine (with some apparent gross errors in a couple of edges). We selected two edges in this image: a "good" edge (in terms of straightness) and a "bad" edge. We determined the datum lines for the good edge and for the bad edge.

An evaluation process influenced by [3] was then employed (see [4] for a detailed description of the experimental methodology. This procedure starts with

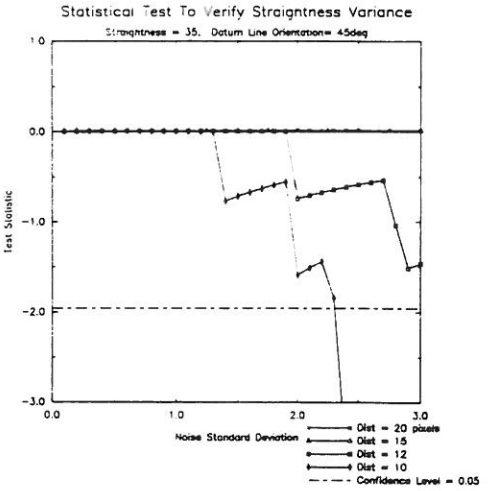

Figure 1: Results of the statistical test to verify straightness variance. The datum line used was oriented at 45^o. The straightness of the synthetic edge used in this test was 35 pixels. The distance between the two edge points that support the datum line was varied from 20 pixels down to 10 pixels. The test fails when the absolute value of the test statistic becomes higher than 1.96 (significance level $\alpha = 0.05$). The test comes close to a breakdown when the distance is 12 pixels (4 times σ) and breaks down when the distance is 10 pixels.

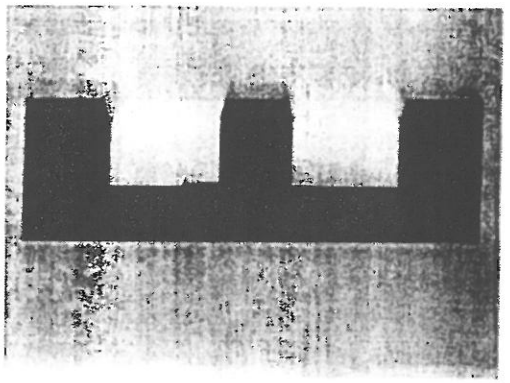

Figure 2: The machined object.

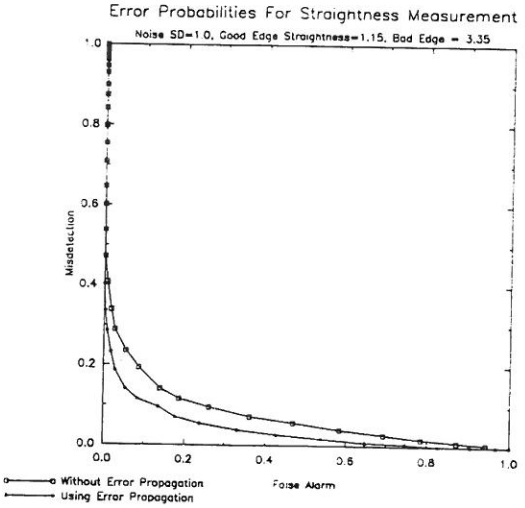

Figure 3: Error probabilities with noise $\sigma = 1.0$.

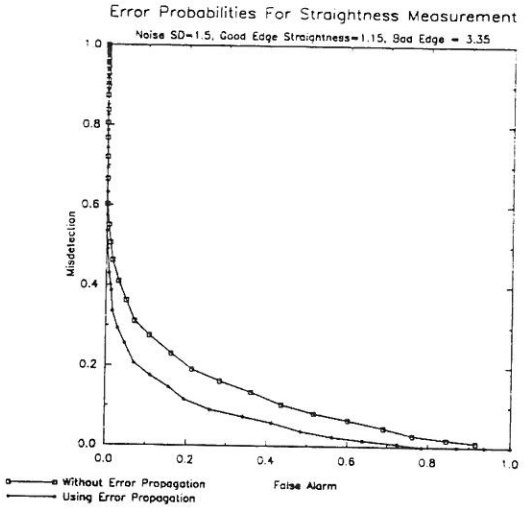

Figure 4: Error probabilities with noise $\sigma = 1.5$.

the real data obtained from the image and performs 1000 different perturbations at each of several noise levels to thoroughly test the procedures. The false alarm and misdetection probabilities we obtained for various noise levels have been plotted in Figures 3 and 4. Our results show that the decision making procedure that takes error propagation into account yields lower error probabilities than the one that does not propagate errors.

6 Conclusions

In this paper, we described a CAD-based machine vision system for dimensional inspection of machined parts. The system performs inspection by strictly adhering to well-defined tolerance definitions. We propagated uncertainties from lower-level edge pixels all the way up to the measurement tasks. We then incorporated these uncertainties in our decision making to rule a feature acceptable or not. Our experimental results verified the uncertainty derivations statistically and also proved that the error probabilities obtained by propagating uncertainties are lower than those obtainable without uncertainty propagation.

This work sets up a theoretical and operational framework for a CAD-based inspection system. Additional measurement tasks can be included by setting up precise tolerance definitions adhering to the guidelines described. Uncertainty propagation for these additional tasks can be done by following the methodology outlined for the straightness of edge task.

References

[1] *American National Standards Institute(ANSI). 1973. Dimensioning and Tolerancing. ANSI Standard Y 14.5.* American Soc. of Mech. Engg., 1973.

[2] F. Etesami and J. Uicker. Automatic dimensional inspection of machine part cross-sections using fourier analysis. *CVGIP*, 29:216–247, 1985.

[3] T. Kanungo, M.Y. Jaisimha, R.M. Haralick, and R. Palmer. An experimental methodology for performance characterization of a line detection algorithm. *SPIE Opt., Illum. and Image sensing for Mach. Vision*, 1385, 1990.

[4] B. R. Modayur. Visual inspection of machined parts. *MSEE Thesis, Dept of EE, Univ. of Wash., Seattle*, 1991.

[5] H.D. Park and O.R. Mitchell. Cad-based planning and execution of inspection. *CVPR*, 1385, 1990.

[6] F.P. Preparata and M.I. Shamos. *Computational Geometry: An Introduction.* Springer- Verlag N.Y. Inc, 1985.

[7] A.A.G. Requicha. Toward a theory of geometric tolerancing. *Intn. Jr. of Rob. Res.*, 2(4):45–60, 1983.

[8] G.A.W. West, T. Fernando, and P.M. Dew. Cad based inspection: Using a vision cell demonstrator. In *IEEE Workshop on Directions in Automated CAD Based Vision*, pages 155–164, 1991.

[9] S. Yi. Illumination control expert for machine vision: A goal driven approach. *PhD Thesis, Dept. of EE, Univ. of Wash.,Seattle*, 1990.